Journal of Applied Analysis and Computation
Volume 11, Number 3, June 2021, 1322–1347
Website:http://www.jaac-online.com
DOI:10.11948/20200158

FLOW OF MAXWELL FLUID IN A CHANNEL WITH UNIFORM POROUS WALLS

Tahira Haroon[1], Abdul Majeed Siddiqui[1], Hameed Ullah[2,3,†] and Dianchen Lu[2]

Abstract In this paper a theoretical study of incompressible Maxwell fluid in a channel with uniform porous walls is presented. Along with the viscoelasticity, inertial effects are also considered. Six nonlinear partial differential equations (PDEs) with non-homogeneous boundary conditions in two dimensions are solved using recursive approach. Expressions for stream function, velocity components, volumetric flow rate, pressure distribution, shear and normal stresses in general and on the walls of the channel, fractional absorption and leakage flux are obtained. The volumetric flow rate and mean flow rate are found to be very useful to understand the flow phenomena through the channel and while defining non-dimensional parameters. Points of maximum velocity components are also identified. A graphical study is carried out to show the effect of absorption, Reynolds number, material parameter on above mentioned resulting expressions. It is observed that velocity of the fluid decreases with the increase in absorption parameter, Reynolds number and also with Maxwell parameter. These results enforce the presence of inertia terms. As all three parameters, mentioned above play very important role in the stability of fluid flow. The limited cases are in full agreement with the available literature. Above mentioned solution technique proved itself a best and easy to handle technique for the solutions of highly nonlinear PDEs with non-homogeneous boundary conditions, a great help to mathematical community. This theoretical study has significant importance in industry and also in biosciences.

Keywords Maxwell fluid, laminar flow, porous walls, constant absorption, recursive approach.

MSC(2010) 76A05, 76A10, 76S99, 76M55.

1. Introduction

Absorption of the fluid from the tubes or channel walls are very important phenomena in geothermal energy extraction, nuclear waste disposal, drying of food, insulation of buildings. Its importance in biomedical engineering can also not be denied. The process of filtration and mass transfer is occurred in the desalination with reverse osmosis, in the circulation of blood through an artificial kidney, that

[†]The corresponding author. Email: ranahameedullah@gmail.com(H. Ullah)
[1]Deparment of Mathematics, Pennsylvania State University, York Campus, 1031 Edgecomb Avenue, York, PA 17403, USA
[2]Faculty of Science, Jiangsu University, Zhenjiang 212013, China
[3]Deparment of Mathematics, COMSATS University Islamabad, Sahiwal Campus, 57000, Pakistan

is, in the haemodialyses in the lymphatic flow in human body through network of lymphatic capillaries and in the flow through renal tubules of nephron in kidneys. Berman [3] has solved Navier-Stokes equations for rectangular duct with two porous walls using similarity along with the perturbation method. Yuan [29], Terril [23,24] and Cox [4] also investigated the flow through porous channel using different techniques. Siddiqui et al. [7,19,20] have published work using channel with different absorption patterns at permeable walls for Stokes problem. Rashevski [16] studied the channel flow by considering one porous wall and investigated the significance impact of heat transfer inside the channel. Recently, Ullah et al [27,28] studied the creeping flow of slightly viscoelastic fluid flows through permeable channel using recursive approach, Kahshan et al [10,11] studied the Micropolar and Jeffery fluid flow through porous walled channel and many authors [1,2,8,22] have also shown keen interest in the channel flow problems with different restrictions.

Biological fluids are not simple fluids, they contain different types of minerals, proteins, like sodium, calcium, potassium, hydrogen, ammonium, magnesium etc.. In the kidneys where filtration, absorption and reabsorption of the fluid occur and urine as a bi product is obtained, fluid cannot be considered as Newtonian. Lots of constitutive models are proposed by the researchers. Few of these models are developed from the classical theory but mostly are based on experimental data, which are known as empirical models. But, per our knowledge, no such constitutive model exists which can define such type of fluids, completely. So one of the reasons for investigation is to find the appropriate model which can fit closely to the experimental data so that using that model we can reach to some useful results for practical purposes. For this purpose we start with a non-Newtonian, viscoelastic rate type fluid model known as Maxwell fluid model, a subclass of Oldroyd fluid model (suggested by Maxwell [15]). Choi et al. [5] discussed the channel flow of Maxwell fluid with suction. A thermodynamic approach for modeling a class of rate type fluids was developed by Rajagopal and Srinivasa [17]. Tan and Xu [25] described the unidirectional flow of viscoelastic fluid with fractional Maxwell model. Sadeghy et al. [21] studied the Sakiadis flow of Maxwell fluid.

We are trying to solve full momentum equations for incompressible Maxwell fluid model, combining the effects of viscoelasticity and inertia in a channel with uniform porous walls. This leads to six two-dimensional highly non-linear partial differential equations along with the non-homogeneous boundary conditions. In general it is very difficult to solve these type of equations either analytically or numerically. Analytical study of such type of nonlinear problem is important not only because of its technological significance but also due to the interesting mathematical features presented by these equations.

Generally, the methods of solution of the nonlinear differential equations are restricted to a variety of special classes of equations and usually involves a limited number of techniques to achieve analytical approximations to the solutions. There are some common approaches for approximating solutions of a non-linear system such as the perturbation methods [6,18] based on an assumption of a small parameter which must exist in the equation, greatly restricting applications of perturbation techniques. In this article we have used a recursive approach proposed by Langlois [12,13]. He used this approach to solve slow viscoelastic fluids flow problems neglecting inertial part. But, we have generalized this approach to solve highly non-linear full two-dimensional momentum equations including inertial part for incompressible Maxwell fluid model along with non-homogeneous boundary con-

ditions. Expressions for the velocity components, flow rate, pressure field, mean pressure drop, wall shear stress, normal stresses, leakage flux and fractional absorption are obtained. Graphical results and discussion are also presented. We hope that this article will be useful in understanding the mechanism of flows through uniform porous boundaries in industry and also in biosciences. This will also attract the mathematical community.

2. Basic Equations

The basic equations governing the steady, laminar flow of an incompressible Maxwell fluid, neglecting thermal effects and body forces are

$$\nabla \cdot \mathbf{V} = 0, \tag{2.1}$$

$$\rho\left[(\mathbf{V}\cdot\nabla)\,\mathbf{V}\right] = -\nabla p + \nabla\cdot\boldsymbol{\tau}, \tag{2.2}$$

where $\mathbf{V}$ is the velocity vector, ρ is the density of the fluid, p is the hydrodynamic pressure and $\boldsymbol{\tau}$ is the extra stress tensor.

Constitutive equation for incompressible Maxwell fluid [5, 14, 21] is:

$$\boldsymbol{\tau} + \lambda \overset{\triangledown}{\boldsymbol{\tau}} = \mu \mathbf{A}_1, \tag{2.3}$$

λ is relaxation time and overhead "$\triangledown$" stands for the contravarient or upper convected derivative, μ is the coefficient of viscosity and $\mathbf{A}_1$ is the first Rivlin-Erickson tensor given by

$$\mathbf{A}_1 = (\nabla\mathbf{V}) + (\nabla\mathbf{V})^T, \tag{2.4}$$

and

$$\overset{\triangledown}{\boldsymbol{\tau}} = (\mathbf{V}\cdot\nabla)\,\boldsymbol{\tau} - \left[(\nabla\mathbf{V})^T\boldsymbol{\tau} + \boldsymbol{\tau}\,(\nabla\mathbf{V})\right], \tag{2.5}$$

where superscript ^{T} denotes the transpose of the given matrix.

3. Problem Statement

We consider steady, laminar, isothermal flow of an incompressible Maxwell fluid through an infinite channel with uniform porous walls. A rectangular Cartesian coordinate system (x, y, z) is chosen with x-axis aligned with the center line of the channel in the direction of flow, and y normal to it. Let the width of the channel be $2H$. The entering volume flow rate Q_0, and absorption velocity $V_\circ$ from the channel walls, are assumed constants. Since channel is considered infinite, the third component of velocity can be neglected and the flow field became two dimensional.

Due to symmetry condition, we choose half of the channel, then the boundary conditions of the problem under consideration (Figure 1) become

$$u = 0, \qquad v = V_\circ, \qquad \text{at} \qquad y = H, \tag{3.1}$$

$$\frac{\partial u}{\partial y} = 0, \qquad v = 0, \qquad \text{at} \qquad y = 0, \tag{3.2}$$

$$Q_0 = \int_{-H}^{H} u(0, y)dy, \tag{3.3}$$

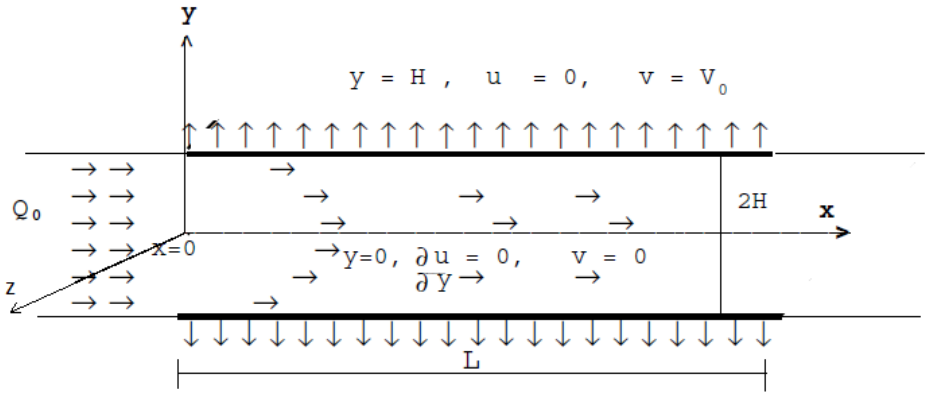

Figure 1. Geometry of the Problem

For steady two-dimensional flow we choose velocity profile of the form

$$\mathbf{V} = [u(x,y), v(x,y)]\,, \tag{3.4}$$

then equations (2.1)–(2.2) reduce to

$$\frac{\partial u}{\partial x} + \frac{\partial v}{\partial y} = 0, \tag{3.5}$$

$$\rho\left[u\frac{\partial u}{\partial x} + v\frac{\partial u}{\partial y}\right] = -\frac{\partial p}{\partial x} + \left[\frac{\partial \tau_{xx}}{\partial x} + \frac{\partial \tau_{xy}}{\partial y}\right], \tag{3.6}$$

$$\rho\left[u\frac{\partial v}{\partial x} + v\frac{\partial v}{\partial y}\right] = -\frac{\partial p}{\partial y} + \left[\frac{\partial \tau_{yx}}{\partial x} + \frac{\partial \tau_{yy}}{\partial y}\right], \tag{3.7}$$

and constitutive equation (2.3) with the help of relations (2.4)–(2.5) becomes

$$\left[1 + \lambda\left(u\frac{\partial}{\partial x} + v\frac{\partial}{\partial y} - 2\frac{\partial u}{\partial x}\right)\right]\tau_{xx} - 2\lambda\tau_{yx}\frac{\partial u}{\partial y} = 2\mu\frac{\partial u}{\partial x}, \tag{3.8}$$

$$\left[1 + \lambda\left(u\frac{\partial}{\partial x} + v\frac{\partial}{\partial y}\right)\right]\tau_{xy} - \lambda\tau_{xx}\frac{\partial v}{\partial x} - \lambda\tau_{yy}\frac{\partial u}{\partial y} = \mu\left[\frac{\partial u}{\partial y} + \frac{\partial v}{\partial x}\right], \tag{3.9}$$

$$\left[1 + \lambda\left(u\frac{\partial}{\partial x} + v\frac{\partial}{\partial y} - 2\frac{\partial v}{\partial y}\right)\right]\tau_{yy} - 2\lambda\tau_{yx}\frac{\partial v}{\partial x} = 2\mu\frac{\partial v}{\partial y}. \tag{3.10}$$

These are six highly non-linear coupled partial differential equations having six unknowns namely, $u(x,y)$, $v(x,y)$, $p(x,y)$, $\tau_{xx}(x,y)$, $\tau_{xy}(x,y)$, $\tau_{yy}(x,y)$, as $\tau_{xy}(x,y) = \tau_{yx}(x,y)$, along with non-homogeneous boundary conditions (3.1)–(3.3). It is still a challenge for researcher community to find exact solution of such type of equations, even finding analytical or numerical solution is very laborious. In the next sections, we will use Langlois recursive approach [12, 13] to find analytical solution of the above system of equations.

4. Solution of the Problem

Following Langlois approach we expand velocity $\mathbf{V}$, pressure p and extra stress tensor $\boldsymbol{\tau}$ as

$$\mathbf{V} = \sum_{i=1}^{\infty} \epsilon^i \ \mathbf{V}^{(i)}, \tag{4.1}$$

$$p = C + \sum_{i=1}^{\infty} \epsilon^i \ p^{(i)}, \tag{4.2}$$

$$\boldsymbol{\tau} = \sum_{i=1}^{\infty} \epsilon^i \ \boldsymbol{\tau}^{(i)}, \tag{4.3}$$

where $\mathbf{V}^{(i)}$, $p^{(i)}$ and $\boldsymbol{\tau}^{(i)}$ are functions of (x, y) only and ϵ is a small, dimensionless constant, C is also a constant. Using expansions (4.1)–(4.3) in equations (3.5)–(3.10) and boundary conditions (3.1)–(3.3), we get:

4.1. First order problem:

Equating the coefficients of ϵ, we obtain

$$\frac{\partial u^{(1)}}{\partial x} + \frac{\partial v^{(1)}}{\partial y} = 0, \tag{4.4}$$

$$\frac{\partial p^{(1)}}{\partial x} = \left[\frac{\partial \tau_{xx}^{(1)}}{\partial x} + \frac{\partial \tau_{xy}^{(1)}}{\partial y} \right], \tag{4.5}$$

$$\frac{\partial p^{(1)}}{\partial y} = \left[\frac{\partial \tau_{yx}^{(1)}}{\partial x} + \frac{\partial \tau_{yy}^{(1)}}{\partial y} \right]. \tag{4.6}$$

Constitutive equations transform to

$$\tau_{xx}^{(1)} = 2\mu \frac{\partial u^{(1)}}{\partial x}, \qquad \tau_{yy}^{(1)} = 2\mu \frac{\partial v^{(1)}}{\partial y}, \quad \tau_{xy}^{(1)} = \mu \left(\frac{\partial u^{(1)}}{\partial y} + \frac{\partial v^{(1)}}{\partial x} \right) \tag{4.7}$$

and the boundary conditions

$$u^{(1)} = 0, \qquad v^{(1)} = V_\circ, \qquad \text{at} \qquad y = H, \tag{4.8}$$

$$\frac{\partial u^{(1)}}{\partial y} = 0, \qquad v^{(1)} = 0, \qquad \text{at} \qquad y = 0, \tag{4.9}$$

$$Q_0^{(1)} = 2 \int_0^H u^{(1)}(0, y) dy. \tag{4.10}$$

Substituting expressions from (4.7) in system of equations (4.5)–(4.6) and using equation of continuity (4.4), we get

$$\frac{\partial p^{(1)}}{\partial x} = \mu \nabla^2 u^{(1)}, \tag{4.11}$$

$$\frac{\partial p^{(1)}}{\partial y} = \mu \nabla^2 v^{(1)}, \tag{4.12}$$

where $\nabla^2 = \dfrac{\partial^2}{\partial x^2} + \dfrac{\partial^2}{\partial y^2}$.

Eliminating pressure from these equations and using stream function

$$u^{(1)} = \frac{\partial \psi^{(1)}}{\partial y}, \qquad v^{(1)} = -\frac{\partial \psi^{(1)}}{\partial x}, \tag{4.13}$$

we reach at

$$\nabla^4 \psi^{(1)} = 0 \tag{4.14}$$

and boundary conditions in term of stream function become

$$\frac{\partial \psi^{(1)}}{\partial y} = 0, \quad \frac{\partial \psi^{(1)}}{\partial x} = -V_\circ, \qquad \text{at} \qquad y = H, \tag{4.15}$$

$$\frac{\partial^2 \psi^{(1)}}{\partial y^2} = 0, \quad \frac{\partial \psi^{(1)}}{\partial x} = 0, \qquad \text{at} \qquad y = 0, \tag{4.16}$$

$$\psi^{(1)}(0, H) = \frac{Q_\circ}{2}, \quad \psi^{(1)}(0, 0) = 0. \tag{4.17}$$

We notice that the problem (4.14)–(4.17) at this order reduces to classical Stokes flow.

Equation (4.14) is a fourth oder partial differential equation. To solve this equation let us assume

$$\psi^{(1)} = xF^{(1)}(y) + G^{(1)}(y), \tag{4.18}$$

where $F^{(1)}(y)$ and $G^{(1)}(y)$ are unknown functions of their arguments. The solution of equation (4.14) using boundary conditions (4.15)–(4.17) become

$$F^{(1)}(y) = -\frac{V_\circ}{2}\left[3\left(\frac{y}{H}\right) - \left(\frac{y}{H}\right)^3\right] \tag{4.19}$$

$$G^{(1)}(y) = \frac{Q_\circ}{4}\left[3\left(\frac{y}{H}\right) - \left(\frac{y}{H}\right)^3\right], \tag{4.20}$$

which after using (4.19) and (4.20) in (4.18), become

$$\psi^{(1)}(x, y) = \frac{1}{2}\left(\frac{Q_\circ}{2} - V_\circ x\right)\left[3\left(\frac{y}{H}\right) - \left(\frac{y}{H}\right)^3\right], \tag{4.21}$$

$$u^{(1)} = \frac{3}{2H}\left(\frac{Q_\circ}{2} - V_\circ x\right)\left[1 - \left(\frac{y}{H}\right)^2\right], \tag{4.22}$$

$$v^{(1)} = \frac{V_\circ}{2}\left[3\left(\frac{y}{H}\right) - \left(\frac{y}{H}\right)^3\right]. \tag{4.23}$$

It can be easily verified that in the absence of porosity, (4.21)–(4.23) reduce to the classical solution of flow between two parallel plates.

4.2. Second order problem:

Equations of motion along with constitutive equation components after collecting terms for coefficients of ϵ^2 are

$$\frac{\partial u^{(2)}}{\partial x} + \frac{\partial v^{(2)}}{\partial y} = 0, \tag{4.24}$$

$$\rho\left[u^{(1)}\frac{\partial u^{(1)}}{\partial x}+v^{(1)}\frac{\partial u^{(1)}}{\partial y}\right]=-\frac{\partial p^{(2)}}{\partial x}+\left[\frac{\partial \tau_{xx}^{(2)}}{\partial x}+\frac{\partial \tau_{xy}^{(2)}}{\partial y}\right], \tag{4.25}$$

$$\rho\left[u^{(1)}\frac{\partial v^{(1)}}{\partial x}+v^{(1)}\frac{\partial v^{(1)}}{\partial y}\right]=-\frac{\partial p^{(2)}}{\partial y}+\left[\frac{\partial \tau_{yx}^{(2)}}{\partial x}+\frac{\partial \tau_{yy}^{(2)}}{\partial y}\right], \tag{4.26}$$

$$\tau_{xx}^{(2)}+\lambda\left[u^{(1)}\frac{\partial \tau_{xx}^{(1)}}{\partial x}+v^{(1)}\frac{\partial \tau_{xx}^{(1)}}{\partial y}-2\tau_{xx}^{(1)}\frac{\partial u^{(1)}}{\partial x}-2\tau_{yx}^{(1)}\frac{\partial u^{(1)}}{\partial y}\right]=2\mu\frac{\partial u^{(2)}}{\partial x}, \tag{4.27}$$

$$\tau_{xy}^{(2)}+\lambda\left[u^{(1)}\frac{\partial \tau_{yx}^{(1)}}{\partial x}+v^{(1)}\frac{\partial \tau_{yx}^{(1)}}{\partial y}-\tau_{xx}^{(1)}\frac{\partial v^{(1)}}{\partial x}-\tau_{yy}^{(1)}\frac{\partial u^{(1)}}{\partial y}\right]=\mu\left[\frac{\partial u^{(2)}}{\partial y}+\frac{\partial v^{(2)}}{\partial x}\right], \tag{4.28}$$

$$\tau_{yy}^{(2)}+\lambda\left[u^{(1)}\frac{\partial \tau_{yy}^{(1)}}{\partial x}+v^{(1)}\frac{\partial \tau_{yy}^{(1)}}{\partial y}-2\tau_{yy}^{(1)}\frac{\partial v^{(1)}}{\partial y}-2\tau_{yx}^{(1)}\frac{\partial v^{(1)}}{\partial x}\right]=2\mu\frac{\partial v^{(2)}}{\partial y}. \tag{4.29}$$

Boundary conditions for the second order problem are now homogeneous at the order of ϵ^2 :

$$u^{(2)}=0, \qquad v^{(2)}=0, \qquad \text{at} \qquad y=H, \tag{4.30}$$

$$\frac{\partial u^{(2)}}{\partial y}=0, \qquad v^{(2)}=0, \qquad \text{at} \qquad y=0, \tag{4.31}$$

$$Q_{\circ}^{(2)}=0. \tag{4.32}$$

Substituting the expressions of $u^{(1)}$, $v^{(1)}$ and their derivatives from (4.22) and (4.23) in system of equation (4.24)–(4.26), we get

$$-\frac{3}{4}\frac{\rho V_{\circ}}{H^2}\left(\frac{Q_{\circ}}{2}-V_{\circ}x\right)\left[3+\left(\frac{y}{H}\right)^4\right]=-\frac{\partial p^{(2)}}{\partial x}+\frac{\partial \tau_{xx}^{(2)}}{\partial x}+\frac{\partial \tau_{xy}^{(2)}}{\partial x}, \tag{4.33}$$

$$\frac{3}{4}\frac{\rho V_{\circ}^2 y}{H^2}\left[3-4\left(\frac{y}{H}\right)^2+\left(\frac{y}{H}\right)^4\right]=-\frac{\partial p^{(2)}}{\partial y}+\frac{\partial \tau_{yx}^{(2)}}{\partial x}+\frac{\partial \tau_{yy}^{(2)}}{\partial x}. \tag{4.34}$$

Eliminating p from these two equations, and substituting from (4.27)–(4.29), and defining stream function as

$$u^{(2)}=\frac{\partial \psi^{(2)}}{\partial y}, \qquad v^{(2)}=-\frac{\partial \psi^{(2)}}{\partial x}, \tag{4.35}$$

we find that the equation (4.24) is satisfied identically and (4.33)–(4.34) reduce to single partial differential equation:

$$-3\frac{\rho V_{\circ}}{H^3}\left(\frac{Q_{\circ}}{2}-V_{\circ}x\right)\left(\frac{y}{H}\right)^3=\mu\nabla^2\left(\nabla^2\psi^{(2)}\right)=\mu\nabla^4\psi^{(2)}. \tag{4.36}$$

Boundary conditions in terms of stream function can be written as

$$\frac{\partial \psi^{(2)}}{\partial y}=0, \quad \frac{\partial \psi^{(2)}}{\partial x}=0, \qquad \text{at} \qquad y=H, \tag{4.37}$$

$$\frac{\partial^2 \psi^{(2)}}{\partial y^2}=0, \quad \frac{\partial \psi^{(2)}}{\partial x}=0, \qquad \text{at} \qquad y=0, \tag{4.38}$$

$$\psi^{(1)}(0,0)=0, \quad \psi^{(1)}(0,H)=0. \tag{4.39}$$

In view of differential equation (4.36) we suggest the solution of this equation of the form

$$\psi^{(2)}=\phi^{(2)}(x)F^{(2)}(y)+G^{(2)}(y), \tag{4.40}$$

where $\phi^{(2)}$ is an unknown linear function of x. Using (4.40) in (4.37)–(4.39), boundary conditions transformed to

$$F^{(2)}(H)=0, \quad F^{(2)}_y(H)=0, \quad F^{(2)}(0)=0, \quad F^{(2)}_{yy}(0)=0, \tag{4.41}$$

$$G^{(2)}(H)=0, \quad G^{(2)}_y(H)=0, \quad G^{(2)}(0)=0, \quad G^{(2)}_{yy}(0)=0. \tag{4.42}$$

Using (4.40) in (4.36) results

$$-3\frac{\rho V_\circ}{H^3}\left(\frac{Q_\circ}{2}-V_\circ x\right)\left(\frac{y}{H}\right)^3=\mu\left[\phi^{(2)}(x)F^{(2)}_{yyyy}(y)+G^{(2)}_{yyyy}(y)\right], \tag{4.43}$$

where the subscripts show the differentiation with respect to y. From (4.43), we can write

$$\phi^{(2)}(x)F^{(2)}_{yyyy}(y)=3R_eV_\circ x\frac{y^3}{H^7}, \qquad G^{(2)}_{yyyy}(y)=-\frac{3}{2}R_eQ_\circ\frac{y^3}{H^7}, \tag{4.44}$$

where $R_e=\dfrac{\rho V_\circ H}{\mu}$ is the Reynolds number.

Let $\phi^{(2)}(x)=3R_eV_\circ x$, then

$$F^{(2)}(y)_{yyyy}=\frac{y^3}{H^7}, \tag{4.45}$$

$$\Rightarrow \qquad F^{(2)}(y)=\frac{1}{840}\frac{y^7}{H^7}+C_1\frac{y^3}{6}+C_2\frac{y^2}{2}+C_3y+C_4. \tag{4.46}$$

Boundary conditions (4.41) lead to

$$F^{(2)}(y)=\frac{1}{840}\left(\frac{y}{H}\right)^7-\frac{1}{280}\left(\frac{y}{H}\right)^3+\frac{1}{420}\left(\frac{y}{H}\right), \tag{4.47}$$

and

$$G^{(2)}(y)_{yyyy}=-\frac{3}{2}R_eQ_\circ\frac{y^3}{H^7},$$

$$\Rightarrow \qquad G(y)=-\frac{1}{560}R_eQ_\circ\frac{y^7}{H^7}+C_5\frac{y^3}{6}+C_6\frac{y^2}{2}+C_7y+C_8. \tag{4.48}$$

Using boundary conditions (4.42) we get

$$G^{(2)}(y)=-\frac{1}{560}R_eQ_\circ\left(\left(\frac{y}{H}\right)^7-3\left(\frac{y}{H}\right)^3+2\left(\frac{y}{H}\right)\right). \tag{4.49}$$

Therefore,

$$\psi^{(2)}(x,y)=-\frac{R_e}{280}\left(\frac{Q_\circ}{2}-V_\circ x\right)\left[\left(\frac{y}{H}\right)^7-3\left(\frac{y}{H}\right)^3+2\left(\frac{y}{H}\right)\right], \tag{4.50}$$

$$u^{(2)}(x,y) = -\frac{R_e}{280H}\left(\frac{Q_\circ}{2} - V_\circ x\right)\left[7\left(\frac{y}{H}\right)^6 - 9\left(\frac{y}{H}\right)^2 + 2\right], \tag{4.51}$$

$$v^{(2)}(x,y) = -\frac{R_e V_\circ}{280}\left[\left(\frac{y}{H}\right)^7 - 3\left(\frac{y}{H}\right)^3 + 2\left(\frac{y}{H}\right)\right]. \tag{4.52}$$

We notice that $\psi^{(2)}(x,y)$, $u^{(2)}(x,y)$ and $v^{(2)}(x,y)$ are contributing in the solution due to the inertial forces otherwise they do not appear in the solution ($R_e = 0$) [26]. It must be noted that up till second order solution the Maxwell material parameter is not contributing.

We have also observed that solutions obtained up till second order using recursive approach are very similar with results obtained by Berman [3] using perturbation method.

4.3. Third order problem:

Equating the coefficients of ϵ^3 from equations of motion along with constitutive equation components, we get system of equations as:

$$\frac{\partial u^{(3)}}{\partial x} + \frac{\partial v^{(3)}}{\partial y} = 0, \tag{4.53}$$

$$\rho\left[u^{(1)}\frac{\partial u^{(2)}}{\partial x} + u^{(2)}\frac{\partial u^{(1)}}{\partial x} + v^{(1)}\frac{\partial u^{(2)}}{\partial y} + v^{(2)}\frac{\partial u^{(1)}}{\partial y}\right] = -\frac{\partial p^{(3)}}{\partial x} + \left[\frac{\partial \tau_{xx}^{(3)}}{\partial x} + \frac{\partial \tau_{xy}^{(3)}}{\partial y}\right], \tag{4.54}$$

$$\rho\left[u^{(1)}\frac{\partial v^{(2)}}{\partial x} + u^{(2)}\frac{\partial v^{(1)}}{\partial x} + v^{(2)}\frac{\partial v^{(1)}}{\partial y} + v^{(1)}\frac{\partial v^{(2)}}{\partial y}\right] = -\frac{\partial p^{(3)}}{\partial y} + \left[\frac{\partial \tau_{yx}^{(3)}}{\partial x} + \frac{\partial \tau_{yy}^{(3)}}{\partial y}\right], \tag{4.55}$$

$$\begin{aligned}\tau_{xx}^{(3)} + \lambda\Bigg[&u^{(1)}\frac{\partial \tau_{xx}^{(2)}}{\partial x} + u^{(2)}\frac{\partial \tau_{xx}^{(1)}}{\partial x} + v^{(1)}\frac{\partial \tau_{xx}^{(2)}}{\partial y} + v^{(2)}\frac{\partial \tau_{xx}^{(1)}}{\partial y} - 2\tau_{xx}^{(2)}\frac{\partial u^{(1)}}{\partial x}\\ &-2\tau_{xx}^{(1)}\frac{\partial u^{(2)}}{\partial x} - 2\tau_{yx}^{(1)}\frac{\partial u^{(2)}}{\partial y} - 2\tau_{yx}^{(2)}\frac{\partial u^{(1)}}{\partial y}\Bigg] = 2\mu\frac{\partial u^{(3)}}{\partial x},\end{aligned} \tag{4.56}$$

$$\begin{aligned}\tau_{xy}^{(3)} + \lambda\Bigg[&u^{(1)}\frac{\partial \tau_{yx}^{(2)}}{\partial x} + u^{(2)}\frac{\partial \tau_{yx}^{(1)}}{\partial x} + v^{(1)}\frac{\partial \tau_{yx}^{(2)}}{\partial y} + v^{(2)}\frac{\partial \tau_{yx}^{(1)}}{\partial y} - \tau_{xx}^{(1)}\frac{\partial v^{(2)}}{\partial x}\\ &-\tau_{xx}^{(2)}\frac{\partial v^{(1)}}{\partial x} - \tau_{yy}^{(1)}\frac{\partial u^{(2)}}{\partial y} - \tau_{yy}^{(2)}\frac{\partial u^{(1)}}{\partial y}\Bigg] = \mu\left[\frac{\partial u^{(3)}}{\partial y} + \frac{\partial v^{(3)}}{\partial x}\right],\end{aligned} \tag{4.57}$$

$$\begin{aligned}\tau_{yy}^{(3)} + \lambda\Bigg[&u^{(1)}\frac{\partial \tau_{yy}^{(2)}}{\partial x} + u^{(2)}\frac{\partial \tau_{yy}^{(1)}}{\partial x} + v^{(1)}\frac{\partial \tau_{yy}^{(2)}}{\partial y} + v^{(2)}\frac{\partial \tau_{yy}^{(1)}}{\partial y} - 2\tau_{yy}^{(1)}\frac{\partial v^{(2)}}{\partial y}\\ &-2\tau_{yy}^{(2)}\frac{\partial v^{(1)}}{\partial y} - 2\tau_{yx}^{(1)}\frac{\partial v^{(2)}}{\partial x} - 2\tau_{yx}^{(2)}\frac{\partial v^{(1)}}{\partial x}\Bigg] = 2\mu\frac{\partial v^{(3)}}{\partial y}.\end{aligned} \tag{4.58}$$

Corresponding boundary conditions

$$u^{(3)} = 0, \qquad v^{(3)} = 0, \qquad \text{at} \qquad y = H, \tag{4.59}$$

$$\frac{\partial u^{(3)}}{\partial y} = 0, \qquad v^{(3)} = 0, \qquad \text{at} \qquad y = 0, \tag{4.60}$$

$$Q_{\circ}^{(3)} = 0. \tag{4.61}$$

Following the same procedure as above, we found

$$\nabla^4\psi^{(3)} = \frac{3}{35}\left(\frac{Q_{\circ}}{2} - V_{\circ}x\right)\left[\frac{R_e^2 y^7}{H^{11}} - \frac{21R_e^2}{2}\frac{y^5}{H^9} + \frac{3}{2}\left(R_e^2 - 70R_e\delta - 560\delta^2\right)\frac{y^3}{H^7}\right] \tag{4.62}$$

where $\delta = \dfrac{\lambda V_{\circ}}{H}$ is the Maxwell material parameter, also known as Deborah number, which characterizes the fluidity of material under specific flow conditions.

Assuming $\psi^{(3)}$ of the form

$$\psi^{(3)} = \phi^{(3)}(x)F^{(3)}(y) + G^{(3)}(y), \tag{4.63}$$

where $\phi^{(3)}$ is a linear function of x and $F^{(3)}$ and $G^{(3)}$ are the functions of y, we obtain

$$\nabla^4\psi^{(3)} = \phi^{(3)}(x)F^{(3)}(y)_{yyyy} + G^{(3)}(y)_{yyyy}. \tag{4.64}$$

Comparing with equation (4.62), we can write

$$\phi^{(3)}(x)F^{(3)}(y)_{yyyy} = -\frac{3}{35}V_{\circ}x\left[\frac{R_e^2 y^7}{H^{11}} - \frac{21R_e^2}{2}\frac{y^5}{H^9} + \frac{3}{2}\left(R_e^2 - 70R_e\delta - 560\delta^2\right)\frac{y^3}{H^7}\right], \tag{4.65}$$

$$G^{(3)}(y)_{yyyy} = \frac{3}{70}Q_{\circ}\left[\frac{R_e^2 y^7}{H^{11}} - \frac{21R_e^2}{2}\frac{y^5}{H^9} + \frac{3}{2}\left(R_e^2 - 70R_e\delta - 560\delta^2\right)\frac{y^3}{H^7}\right], \tag{4.66}$$

and boundary conditions transformed to

$$F^{(3)}(H) = 0, \quad F^{(3)}(H)_y = 0, \quad F^{(3)}(0) = 0, \quad F^{(3)}(0)_{yy} = 0, \tag{4.67}$$

$$G^{(3)}(H) = 0, \quad G^{(3)}(H)_y = 0, \quad G^{(3)}(0) = 0, \quad G^{(3)}(0)_{yy} = 0. \tag{4.68}$$

Let $\phi^{(3)}(x) = -\dfrac{3}{35}V_{\circ}x$ then

$$F^{(3)}(y)_{yyyy} = \frac{R_e^2 y^7}{H^{11}} - \frac{21R_e^2}{2}\frac{y^5}{H^9} + \frac{3}{2}\left(R_e^2 - 70R_e\delta - 560\delta^2\right)\frac{y^3}{H^7}\Bigg). \tag{4.69}$$

Integrating equation (4.69) four times with respect to y gives

$$\begin{aligned} F^{(3)}(y) = &\frac{R_e^2}{7920}\left(\frac{y}{H}\right)^{11} - \frac{R_e^2}{288}\left(\frac{y}{H}\right)^{9} - \left(\delta^2 + \frac{R_e\delta}{8} - \frac{R_e^2}{560}\right)\left(\frac{y}{H}\right)^{7} \\ &+ C_{13}\frac{y^3}{6} + C_{14}\frac{y^2}{2} + C_{15}y + C_{16}, \end{aligned} \tag{4.70}$$

and integrating equation (4.66) four times with respect to y gives

$$\begin{aligned} G(y) = &\frac{3}{70}Q_{\circ}\left\{\frac{1}{7920}\left(\frac{y}{H}\right)^{11} - \frac{1}{288}\left(\frac{y}{H}\right)^{9} - \left(\delta^2 + \frac{\delta}{8} - \frac{1}{560}\right)\left(\frac{y}{H}\right)^{7}\right. \\ &\left. + C_{17}\frac{y^3}{6} + C_{18}\frac{y^2}{2} + C_{19}y + C_{20}\right\}. \end{aligned} \tag{4.71}$$

Using above boundary conditions we get

$$F^{(3)}(y) = \frac{R_e^2}{7920}\left(\frac{y}{H}\right)^{11} - \frac{R_e^2}{288}\left(\frac{y}{H}\right)^{9} - \left(\delta^2 + \frac{R_e}{8}\,\delta - \frac{R_e^2}{560}\right)\left(\frac{y}{H}\right)^{7} + \left(3\,\delta^2 + \frac{3}{8}\,\delta R_e + \frac{73R_e^2}{9240}\right)\left(\frac{y}{H}\right)^{3} - \left(2\,\delta^2 + \frac{1}{4}\,\delta R_e + \frac{703R_e^2}{110880}\right)\left(\frac{y}{H}\right), \tag{4.72}$$

$$G^{(3)}(y) = \frac{3}{70}Q_\circ\left[\frac{R_e^2}{7920}\left(\frac{y}{H}\right)^{11} - \frac{R_e^2}{288}\left(\frac{y}{H}\right)^{9} - \left(\delta^2 + \frac{R_e}{8}\,\delta - \frac{R_e^2}{560}\right)\left(\frac{y}{H}\right)^{7} + \left(3\,\delta^2 + \frac{3}{8}\,\delta R_e + \frac{73R_e^2}{9240}\right)\left(\frac{y}{H}\right)^{3} - \left(2\,\delta^2 + \frac{1}{4}\,\delta R_e + \frac{703R_e^2}{110880}\right)\left(\frac{y}{H}\right)\right]. \tag{4.73}$$

Therefore, relation (4.63) transformed to

$$\psi^{(3)}(x,y) = \frac{3}{35}\left(\frac{Q_\circ}{2} - xV_\circ\right)\left[\frac{R_e^2}{7920}\left(\frac{y}{H}\right)^{11} - \frac{R_e^2}{288}\left(\frac{y}{H}\right)^{9} - \left(\delta^2 + \frac{1}{8}\,\delta R_e - \frac{R_e^2}{560}\right)\left(\frac{y}{H}\right)^{7} + \left(3\,\delta^2 + \frac{3}{8}\,\delta R_e + \frac{73R_e^2}{9240}\right)\left(\frac{y}{H}\right)^{3} - \left(2\,\delta^2 + \frac{1}{4}\,\delta R_e + \frac{703R_e^2}{110880}\right)\left(\frac{y}{H}\right)\right]. \tag{4.74}$$

$$u^{(3)}(x,y) = \frac{3}{35\,H}\left(\frac{Q_\circ}{2} - V_\circ x\right)\left[\frac{R_e^2}{720}\left(\frac{y}{H}\right)^{10} - \frac{R_e^2}{32}\left(\frac{y}{H}\right)^{8} - \left(7\delta^2 + \frac{7}{8}\delta R_e - \frac{R_e^2}{80}\right)\left(\frac{y}{H}\right)^{6} + \left(9\delta^2 + \frac{9}{8}\delta R_e + \frac{73R_e^2}{3080}\right)\left(\frac{y}{H}\right)^{2} - \left(2\delta^2 + \frac{1}{4}\delta R_e + \frac{703R_e^2}{110880}\right)\right]. \tag{4.75}$$

$$v^{(3)}(x,y) = \frac{3}{35}\,V_\circ\left[\frac{R_e^2}{7920}\left(\frac{y}{H}\right)^{11} - \frac{R_e^2}{288}\left(\frac{y}{H}\right)^{9} - \left(\delta^2 + \frac{1}{8}\,\delta R_e - \frac{R_e^2}{560}\right)\left(\frac{y}{H}\right)^{7} + \left(3\,\delta^2 + \frac{3}{8}\,\delta R_e + \frac{73R_e^2}{9240}\right)\left(\frac{y}{H}\right)^{3} - \left(2\,\delta^2 + \frac{1}{4}\,\delta R_e + \frac{703R_e^2}{110880}\right)\left(\frac{y}{H}\right)\right]. \tag{4.76}$$

Ultimately, we get

$$\psi(x,y) = \frac{1}{35}\left(\frac{Q_\circ}{2} - V_\circ x\right)\left[\frac{R_e^2}{2640}\left(\frac{y}{H}\right)^{11} - \frac{R_e^2}{96}\left(\frac{y}{H}\right)^{9} - \left\{3\delta^2 + \left(\frac{3\delta}{8} + \frac{1}{8}\right)R_e - \frac{3R_e^2}{560}\right\}\left(\frac{y}{H}\right)^{7} + \left\{9\delta^2 + \frac{3}{8}(3\delta+1)R_e + \frac{73R_e^2}{3080} - \frac{35}{2}\right\}\left(\frac{y}{H}\right)^{3} - \left\{6\delta^2 + \frac{1}{4}(3\delta+1)R_e + \frac{703R_e^2}{36960} - \frac{105}{2}\right\}\left(\frac{y}{H}\right)\right]. \tag{4.77}$$

$$u(x,y) = \frac{1}{35H}\left(\frac{Q_\circ}{2} - V_\circ x\right)\left[\frac{R_e^2}{240}\left(\frac{y}{H}\right)^{10} - \frac{3}{32}R_e^2\left(\frac{y}{H}\right)^{8}\right.$$

$$
\begin{aligned}
&- 7\left\{3\delta^2+\left(\frac{3\delta}{8}+\frac{1}{8}\right)R_e-\frac{3R_e^2}{560}\right\}\left(\frac{y}{H}\right)^6\\
&+3\left\{9\delta^2+\frac{3}{8}(3\delta+1)R_e+\frac{73R_e^2}{3080}-\frac{35}{2}\right\}\left(\frac{y}{H}\right)^2\\
&-\left\{6\delta^2+\frac{1}{4}(3\delta+1)R_e+\frac{703R_e^2}{36960}-\frac{105}{2}\right\}\Bigg]. \qquad (4.78)
\end{aligned}
$$

$$
\begin{aligned}
v(x,y)=&\frac{V_\circ}{35}\left[\frac{R_e^2}{2640}\left(\frac{y}{H}\right)^{11}-\frac{R_e^2}{96}\left(\frac{y}{H}\right)^9\right.\\
&-\left\{3\delta^2+\left(\frac{3\delta}{8}+\frac{1}{8}\right)R_e-\frac{3R_e^2}{560}\right\}\left(\frac{y}{H}\right)^7\\
&+\left\{9\delta^2+\frac{3}{8}(3\delta+1)R_e+\frac{73R_e^2}{3080}-\frac{35}{2}\right\}\left(\frac{y}{H}\right)^3\\
&-\left.\left\{6\delta^2+\frac{1}{4}(3\delta+1)R_e+\frac{703R_e^2}{36960}-\frac{105}{2}\right\}\left(\frac{y}{H}\right)\right]. \qquad (4.79)
\end{aligned}
$$

Volumetric flow rate is calculated as

$$Q(x)=Q_\circ-2V_\circ x. \qquad (4.80)$$

The maximum axial velocity occurs at the center of the channel

$$u_{max}=-\frac{Q(x)}{70H}\left[6\delta^2+\frac{1}{4}(3\delta+1)R_e+\frac{703R_e^2}{36960}-\frac{105}{2}\right]. \qquad (4.81)$$

Transverse velocity

$$v=0 \qquad \text{at} \qquad y=0,$$

and

$$v=V_\circ \qquad \text{at} \qquad y=H.$$

Pressure is calculated using equation (4.11)–(4.12)

$$\frac{\partial p^{(1)}}{\partial x}=-\frac{3\mu}{H^3}\left(\frac{1}{2}Q_\circ-V_\circ x\right), \qquad (4.82)$$

$$\frac{\partial p^{(1)}}{\partial y}=-\frac{3\mu}{H^3}V_\circ y. \qquad (4.83)$$

Integrating equation (4.82) with respect to x gives

$$p^{(1)}=-\frac{3\mu}{2H^3}\left(Q_\circ x-V_\circ x^2\right)+A\left(y\right). \qquad (4.84)$$

Now differentiating with respect to y, and comparing with the equation (4.83), yields

$$\frac{d}{dy}A\left(y\right)=-\frac{3\mu\, V_\circ y}{H^3}, \qquad (4.85)$$

which implies

$$p^{(1)}=-\frac{3\mu}{2H^3}\left(Q_\circ-V_\circ x\right)x-\frac{3\mu V_\circ y^2}{2H^3}+p_\circ^{(1)}, \qquad (4.86)$$

where $p_\circ^{(1)} = p^{(1)}(0,0)$ is the pressure at the entrance of the channel at $(x,y) = (0,0)$.

The mean pressure drop $\bar{p}$ at any position in channel can be obtained from the formula

$$\begin{aligned}\bar{p}^{(1)} &= \frac{1}{H}\int_0^H \left[p^{(1)} - p_\circ^{(1)}\right] dy,\\ &= -\frac{\mu}{2H}\left[\frac{3\left(Q_\circ - V_\circ x\right)x}{H^2} + V_\circ\right].\end{aligned} \tag{4.87}$$

Similarly, we can obtain

$$\begin{aligned}p^{(2)} - p_\circ^{(2)} =& \frac{\mu V_\circ}{H}\left[-\frac{3R_e}{20}\left(\frac{y}{H}\right)^6 + \left(3\delta + \frac{3R_e}{4}\right)\left(\frac{y}{H}\right)^4 + \left(-\frac{9\delta}{2} - \frac{153R_e}{140}\right)\right.\\ &\left.\times\left(\frac{y}{H}\right)^2 + \left(\frac{9\delta}{2} - \frac{81R_e}{70}\right)\left(\frac{x^2}{H^2} - \frac{xQ_\circ}{H^2 v_\circ}\right)\right],\end{aligned} \tag{4.88}$$

$$\bar{p}^{(2)} = \frac{\mu V_\circ}{H}\left[\frac{-3}{140}\left(42\delta + 11R_e\right) + \left(\frac{9\delta}{2} - \frac{81R_e}{70}\right)\left(\frac{x^2}{H^2} - \frac{xQ_\circ}{H^2 v_\circ}\right)\right], \tag{4.89}$$

$$\begin{aligned}p^{(3)} - p_\circ^{(3)} =& \frac{\mu V_\circ}{H}\left[-\frac{R_e^2}{600}\left(\frac{y}{H}\right)^{10} + \left(\frac{3R_e\left(24\delta + R_e\right)}{1120}\right)\left(\frac{y}{H}\right)^8\right.\\ &+ \left(\frac{9R_e^2}{1400} - \frac{18\delta^2}{5}\right)\left(\frac{y}{H}\right)^6 + \left(-\frac{9\delta R_e}{70} - \frac{1}{560}11R_e^2\right)\left(\frac{y}{H}\right)^4\\ &+ \left(-\frac{891\delta^2}{70} + \frac{3\delta R_e}{14} + \frac{687R_e^2}{53900}\right)\left(\frac{y}{H}\right)^2\\ &\left.+ \left(-\frac{891\delta^2}{70} + \frac{3\delta R_e}{14} - \frac{117R_e^2}{13475}\right)\left(\frac{xQ_\circ}{H^2 v_\circ} - \frac{x^2}{H^2}\right)\right],\end{aligned} \tag{4.90}$$

$$\begin{aligned}\bar{p}^{(3)} =& \frac{\mu V_\circ}{H}\left[-\frac{333\delta^2}{70} + \frac{37\delta R_e}{700} + \frac{597R_e^2}{431200}\right.\\ &\left.+ \left(-\frac{891\delta^2}{70} + \frac{3\delta R_e}{14} - \frac{117R_e^2}{13475}\right)\left(\frac{xQ_\circ}{H^2 v_\circ} - \frac{x^2}{H^2}\right)\right].\end{aligned} \tag{4.91}$$

Total pressure difference is then obtained as

$$\begin{aligned}\Delta p &= p - p_\circ,\\ &= \left(p^{(1)} + p^{(2)} + p^{(3)} + \cdots\right) - \left(p_\circ^{(1)} + p_\circ^{(2)} + p_\circ^{(3)} + \cdots\right).\end{aligned} \tag{4.92}$$

The wall shear stress is obtained as

$$\begin{aligned}\tau_w = -\tau_{xy}\big|_{y=H} =& \frac{\mu}{35\ H^2}\left(\frac{Q_\circ}{2} - V_\circ x\right)\\ &\left[1647\delta^2 - 105\delta + (3 - 15\delta)R_e + \frac{394R_e^2}{1155} + 105\right],\end{aligned} \tag{4.93}$$

which decays from entrance to exit of the channel.

The fractional absorption in a length L is defined as

$$F_a = \frac{Q_\circ - Q_L}{Q_\circ} = \frac{2V_\circ L}{Q_\circ}. \tag{4.94}$$

The leakage flux $q(x)$ is defined as

$$q(x) = -\frac{dQ}{dx} = 2V_\circ. \tag{4.95}$$

Normal stresses are given by

$$\begin{aligned}\tau_{xx} - \tau_{yy} =& \frac{\mu V_\circ}{H}\left[-\frac{R_e^2}{2100}\left(\frac{y}{H}\right)^{10} + \left(\frac{3}{280}R_e\left(32\delta + R_e\right)\right)\left(\frac{y}{H}\right)^8\right.\\ &+\left\{\frac{342\delta^2}{5} + \frac{1}{10}(1-6\delta)R_e - \frac{3R_e^2}{700} + \frac{9\delta R_e\left(Q_\circ - 2xv_\circ\right)^2}{20H^2v_\circ^2}\right\}\left(\frac{y}{H}\right)^6\\ &+\left\{-216\delta^2 + 6\delta - \frac{9\delta R_e}{35} - \frac{27\delta^2\left(Q_\circ - 2xv_\circ\right)^2}{2H^2v_\circ^2}\right\}\left(\frac{y}{H}\right)^4\\ &+\left\{6 - 18\delta + \frac{7452\delta^2}{35} + \frac{3}{70}(2\delta - 3)R_e - \frac{219R_e^2}{26950}\right.\\ &\left.-\frac{9\delta\left(3R_e - 70\right)\left(Q_\circ - 2xv_\circ\right)^2}{140H^2v_\circ^2}\right\}\left(\frac{y}{H}\right)^2\\ &\left.-6 - \frac{1866\delta^2}{35} + \frac{1}{35}(3\delta + 1)R_e + \frac{703R_e^2}{323400}\right].\end{aligned} \tag{4.96}$$

Normal stresses at the wall and at the center of the channel are given by

$$\begin{aligned}\tau_{xx} - \tau_{yy}\Big|_{y=H} =& \frac{\mu V_\circ}{H}\left[\left(12(\delta-1)\delta - \frac{12\delta R_e}{35}\right)\right.\\ &\left.-\left(\frac{9\delta\left(105\delta - 2R_e - 35\right)\left(Q_\circ - 2xv_\circ\right)^2}{70H^2v_\circ^2}\right)\right],\end{aligned} \tag{4.97}$$

$$\tau_{xx} - \tau_{yy}\Big|_{y=0} = \frac{\mu V_\circ}{H}\left[-6 - \frac{1866\delta^2}{35} + \frac{1}{35}(3\delta+1)R_e + \frac{703R_e^2}{323400}\right]. \tag{4.98}$$

5. Non-dimensional form of Solution

The expression obtained for volumetric flow rate (4.80) suggest us that $\dfrac{2V_\circ x}{Q_\circ}$ must be less than one otherwise back flow will occur, therefore, we define non-dimensional parameters of the form

$$\begin{aligned} x^* &= \frac{x}{H}, \qquad & \xi &= \frac{y}{H}, \qquad & u^* &= \frac{u}{Q_\circ/H},\\ v^* &= \frac{v}{Q_\circ/H}, \qquad & \psi^* &= \frac{\psi}{Q_\circ}, \end{aligned} \tag{5.1}$$

then equations (4.77)–(4.79) transformed to

$$\begin{aligned}\psi^* =& \frac{1}{70}\left(1 - Sx^*\right)\left[\frac{R_e^2}{2640}\,\xi^{11} - \frac{R_e^2}{96}\,\xi^9 - \left\{3\delta^2 + \left(\frac{3\delta}{8} + \frac{1}{8}\right)R_e - \frac{3R_e^2}{560}\right\}\,\xi^7\right.\\ &+\left\{9\delta^2 + \frac{3}{8}(3\delta+1)R_e + \frac{73R_e^2}{3080} - \frac{35}{2}\right\}\,\xi^3\\ &\left.-\left\{6\delta^2 + \frac{1}{4}(3\delta+1)R_e + \frac{703R_e^2}{36960} - \frac{105}{2}\right\}\,\xi\right],\end{aligned} \tag{5.2}$$

$$
\begin{aligned}
u^* =& \frac{1}{70}\left(1-Sx^*\right)\left[\frac{R_e^2}{240}\,\xi^{10}-\frac{3}{32}R_e^2\,\xi^8-7\left\{3\delta^2+\left(\frac{3\delta}{8}+\frac{1}{8}\right)R_e-\frac{3R_e^2}{560}\right\}\,\xi^6\right.\\
&+3\left\{9\delta^2+\frac{3}{8}(3\delta+1)R_e+\frac{73R_e^2}{3080}-\frac{35}{2}\right\}\,\xi^2\\
&\left.-\left\{6\delta^2+\frac{1}{4}(3\delta+1)R_e+\frac{703R_e^2}{36960}-\frac{105}{2}\right\}\right], \qquad (5.3)\\
v^* =& \frac{S}{70}\left[\frac{R_e^2}{2640}\,\xi^{11}-\frac{R_e^2}{96}\,\xi^9-\left\{3\delta^2+\left(\frac{3\delta}{8}+\frac{1}{8}\right)R_e-\frac{3R_e^2}{560}\right\}\,\xi^7\right.\\
&+\left\{9\delta^2+\frac{3}{8}(3\delta+1)R_e+\frac{73R_e^2}{3080}-\frac{35}{2}\right\}\,\xi^3\\
&\left.-\left\{6\delta^2+\frac{1}{4}(3\delta+1)R_e+\frac{703R_e^2}{36960}-\frac{105}{2}\right\}\,\xi\right], \qquad (5.4)
\end{aligned}
$$

where dimensionless parameters S, τ_{ij}^*, and p^* are the absorption parameter, stresses and pressure, respectively, given by

$$
S=\frac{2V_\circ H}{Q_\circ}, \qquad \tau_{ij}^*=\frac{\tau_{ij}}{\mu V_\circ/H}, \qquad p^*=\frac{p-p_\circ}{\mu V_\circ/H}. \qquad (5.5)
$$

Therefore, we obtain skin friction as:

$$
\tau_w^*=\frac{\left(1-Sx^*\right)}{35S}\left[1647\delta^2-105\delta+(3-15\delta)R_e+\frac{394R_e^2}{1155}+105\right]. \qquad (5.6)
$$

Normal stresses difference between two porous walls is calculated as

$$
\begin{aligned}
\tau_{xx}^*-\tau_{\xi\xi}^* =& \left[-\frac{R_e^2}{2100}\,\xi^{10}+\left(\frac{3}{280}R_e\left(32\delta+R_e\right)\right)\,\xi^8\right.\\
&+\left\{\frac{342\delta^2}{5}+\frac{1}{10}(1-6\delta)R_e-\frac{3R_e^2}{700}+\frac{9\delta R_e\left(1-Sx^*\right)^2}{5S^2}\right\}\,\xi^6\\
&+\left\{-216\delta^2+6\delta-\frac{9\delta R_e}{35}-\frac{54\delta^2\left(1-Sx^*\right)^2}{S^2}\right\}\,\xi^4\\
&+\left\{6-18\delta+\frac{7452\delta^2}{35}+\frac{3}{70}(2\delta-3)R_e-\frac{219R_e^2}{26950}\right.\\
&\left.-\frac{9\delta\left(3R_e-70\right)\left(1-Sx^*\right)^2}{35S^2}\right\}\,\xi^2-6-\frac{1866\delta^2}{35}\\
&\left.+\frac{1}{35}(3\delta+1)R_e+\frac{703R_e^2}{323400}\right], \qquad (5.7)\\
\tau_{xx}^*-\tau_{\xi\xi}^*\Big|_{\xi=1} =& \left[\left(12(\delta-1)\delta-\frac{12\delta R_e}{35}\right)\right.\\
&\left.-\left(\frac{18\delta\left(105\delta-2R_e-35\right)\left(1-Sx^*\right)^2}{35S^2}\right)\right], \qquad (5.8)\\
\tau_{xx}^*-\tau_{\xi\xi}^*\Big|_{\xi=0} =& \left[-6-\frac{1866\delta^2}{35}+\frac{1}{35}(3\delta+1)R_e+\frac{703R_e^2}{323400}\right]. \qquad (5.9)
\end{aligned}
$$

Expressions (5.8) and (5.9) are the normal stresses differences at the upper wall and at the center of the channel, respectively.

Pressure difference in non-dimensional form becomes

$$\begin{aligned}\Delta p^* =& \frac{-R_e^2}{600}\,\xi^{10} + \left(\frac{3R_e\,(24\delta + R_e)}{1120}\right)\,\xi^8 + \left(-\frac{18\delta^2}{5} + \frac{9R_e^2}{1400} - \frac{3R_e}{20}\right)\,\xi^6 \\ &+ \left(3\delta + \left(\frac{3}{4} - \frac{9\delta}{70}\right)R_e - \frac{1}{560}11R_e^2\right)\,\xi^4 \\ &+ \left(-\frac{3}{2} - \frac{891\delta^2}{70} - \frac{9\delta}{2}\delta + \frac{3}{140}(10-51)R_e + \frac{687R_e^2}{53900}\right)\,\xi^2 \\ &+ \left(\frac{3}{2} + \frac{891\delta^2}{70} + \frac{9\delta}{2} - \frac{3}{70}(5\delta + 27)R_e + \frac{117R_e^2}{13475}\right)\left((x^*)^2 - \frac{2x^*}{S}\right). \quad (5.10)\end{aligned}$$

6. Results and discussion

Analytical solution of full momentum equations for incompressible Maxwell fluid between two porous walls is obtained. The expressions for velocity components, streamlines, pressure distribution, normal and shear stresses, skin friction, volumetric flow rate, fractional absorption and leakage flux are calculated. Their behavior at different positions in the channel with the change in absorption parameter S, Maxwell fluid parameter δ, Reynolds number R_e, are discussed and also presented graphically. The mathematical expression obtained for volumetric flow rate equation (4.80) suggest that forward flow is possible only if $Q(x) > 0$, otherwise back flow will occur. Keeping this consideration in mind, we defined dimensionless absorption parameter $S = \dfrac{2V_\circ H}{Q_\circ}$, such that S must be less than 1 to maintain forward flow i.e., to get $Q(x) > 0$. We non-dimensionlized equations, keeping physics of the problem in mind using parameters given by equations (5.1) and (5.5).

Figures 2(a–c) are showing the variation in u, axial velocity component of creeping Newtonian fluid ($R_e = 0$) at different positions along the channel with changing S. we notice that when there is no porosity ($S = 0$) the same parabolic profile (Poiseuille flow) is obtained through out the channel, but by introducing the porosity, magnitude of u is decreasing and also it is decreasing downstream [19]. Figures

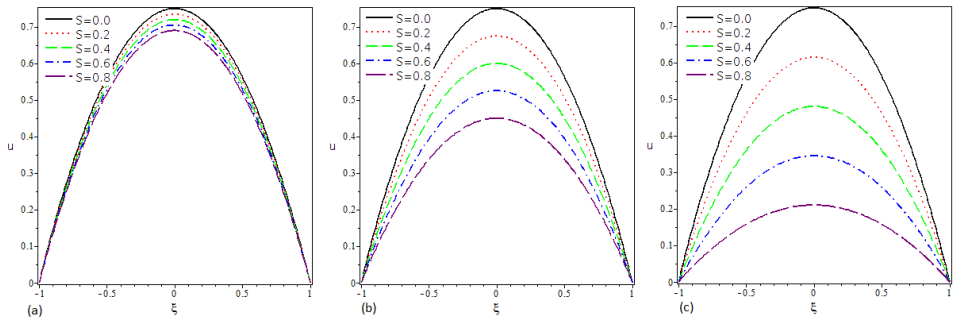

Figure 2. Variation in axial velocity due to absorption S when $R_e = 0$, $\delta = 0$, at (a) $x = 0.1$, (b) $x = 0.5$, (c) $x = 0.9$

3(a–c) show the graphs of u when $R_e = 15$ for Newtonian fluid at different positions along the flow channel with changing S. We noticed the reduction in the

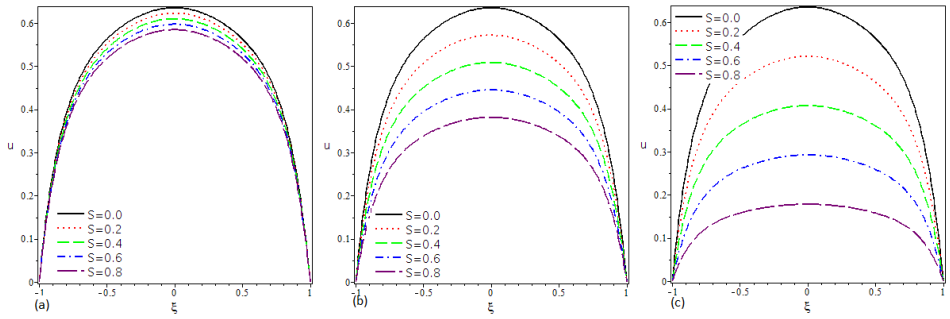

Figure 3. Variation in axial velocity due to absorption when $R_e = 15$, $\delta = 0$, at (a) $x = 0.1$, (b) $x = 0.5$, (c) $x = 0.9$

magnitude of u, flattening near the centerline (effect of boundary is reducing) and increase in the boundary layer thickness due to absorption (increasing porosity). By introducing porosity, parabolicity is diminishing along the channel.

Figures 4(a–c) are drawn to show the variation in u at different axial positions due to δ, Maxwell material parameter (Deborah number). For Newtonian fluid, ($\delta = 0$) keeping $S = 0.4$ and $R_e = 15$, we observe that u is decreasing with increasing δ and it is also reducing downstream. By increasing the value of δ (from 0 to 0.4), a transition of fluid from Newtonian to non-Newtonian can be observed. As it becomes non-Newtonian (Maxwell), fluid moves faster near the walls as compared to the position near the center line, we can observe decrease in the magnitude of u in the central region. Also, decreasing boundary layer thickness can be noticed. This behavior of slow down the velocity, is showing thickening behavior of Maxwell fluid, which is realistic in nature [9].

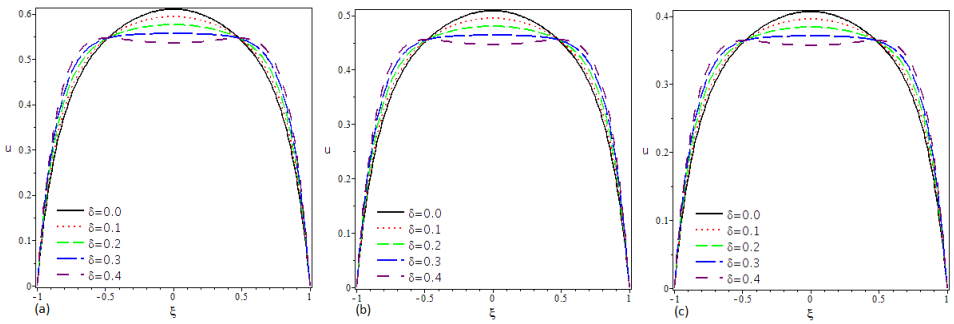

Figure 4. Variation in axial velocity due to δ when $R_e = 15$, $S = 0.4$, at (a) $x = 0.1$, (b) $x = 0.5$, (c) $x = 0.9$

In figures 5(a–c) and 6(a–c) variation in u with S for Maxwell fluid with $\delta = 0.4$ and two different Reynolds numbers i.e., $R_e = 5$ and $R_e = 15$, can be observed at different axial positions in the channel. A comparison between u profiles of Newtonian and Maxwell fluids downstream due to S when $R_e = 15$ can also be drawn from figs. 3(a–c) and 6(a–c). These figures are showing shear thickening behavior. It can be clearly seen from figs. 6(a–c) that with increasing R_e fluid

velocity increases near the walls but thick fluidity causes reduction in u in the central region. With increasing R_e, 6(a–c), plug flow then slow flow in the central region of the channel can be observed.

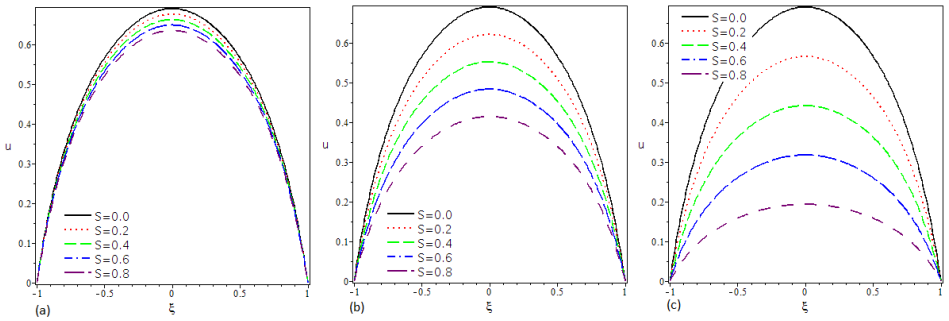

Figure 5. Variation in axial velocity due to S when $R_e = 5$, $\delta = 0.4$, at (a) $x = 0.1$, (b) $x = 0.5$, (c) $x = 0.9$

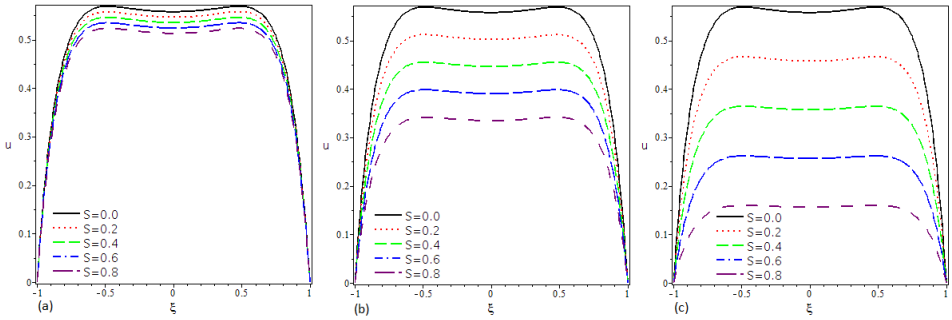

Figure 6. Variation in axial velocity due to S when $R_e = 15$, $\delta = 0.4$, at (a) $x = 0.1$, (b) $x = 0.5$, (c) $x = 0.9$

In figs. 7(a–c) we can compare the effect of R_e on u for Newtonian fluid (a) without porosity (b) with porosity and Maxwell fluid (c) without porosity. In figs. 7(a–b) we see decrease in u with the increase in porosity. With the increase in Reynolds number, in both cases (with and without porosity) boundary layer thickness is decreasing (u near the boundaries is increasing) but the effect of boundaries is decreasing toward central region. We observe from Figs. 7(a–c), shear thickening behavior of Maxwell fluid, even back flow at higher Reynolds number can be observed for Maxwell fluid.

Figs. 8(a–c) and 9(a–c) are showing the effect of porosity at different positions in the channel on Newtonian and Maxwell fluids, respectively for different R_e numbers. In the case of Newtonian fluid we see reduction in u in the central region but no back flow. For Maxwell fluid, we noticed the back flow for the same values of Reynolds number, the thickening behavior.

Figs. 10(a–c) are showing the effect of R_e on u for Maxwell fluid in porous channel for $\delta = 0.2$ and $S = 0.4$ at different positions downstream the channel. We observe that boundary layer thickness is decreasing in Maxwell fluid as compare to Newtonian fluid under the same conditions. Here, once again thickening behavior

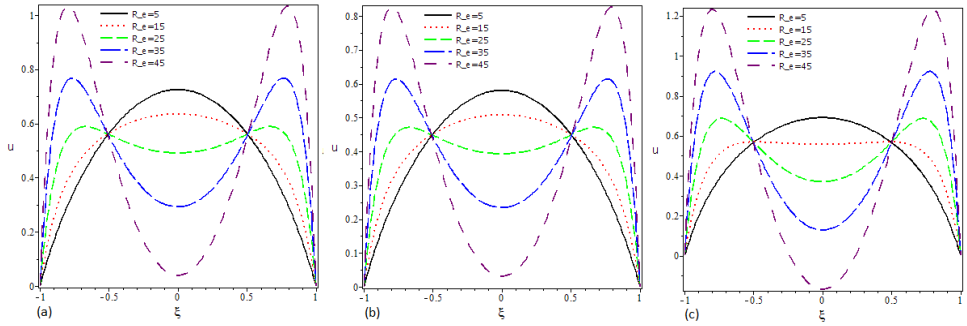

Figure 7. Variation in axial velocity at $x = 0.5$ due to R_e when (a) $S = 0.0,\ \delta = 0.0$, (b) $S = 0.4,\ \delta = 0.0$, (c) $S = 0.0,\ \delta = 0.4$.

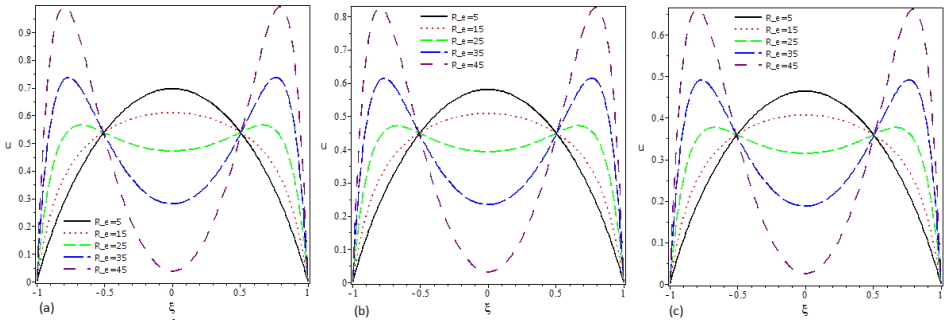

Figure 8. Variation in axial velocity due to R_e when $S = 0.4,\ \delta = 0.0$, at (a) $x = 0.1$, (b) $x = 0.5$, (c) $x = 0.9$

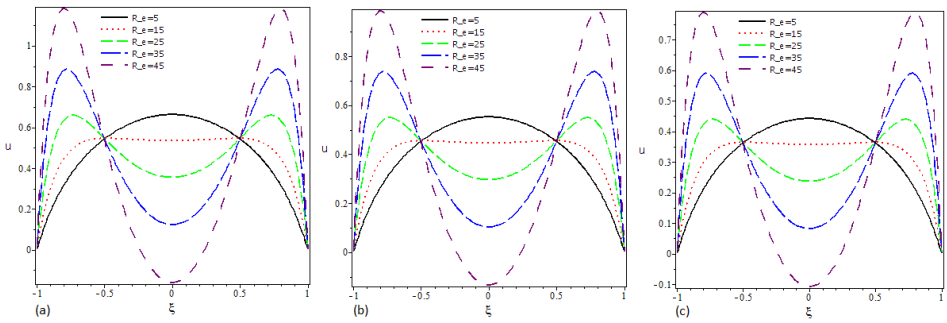

Figure 9. Variation in axial velocity due to R_e when $S = 0.4,\ \delta = 0.4$, at (a) $x = 0.1$, (b) $x = 0.5$, (c) $x = 0.9$

of Maxwell fluid is confirmed.

Figs. 11(a–c) are showing the change in radial velocity profile v for Newtonian and Maxwell fluids due to S when $R_e = 45$ and (a) $\delta = 0.0$ (b) $\delta = 0.4$ (c) $\delta = 0.8$ while in figs. 12(a–c) the effect of S on v when $\delta = 0.4$ and (a) $R_e = 5$ (b) $R_e = 25$ (c) $R_e = 45$ can be noticed.

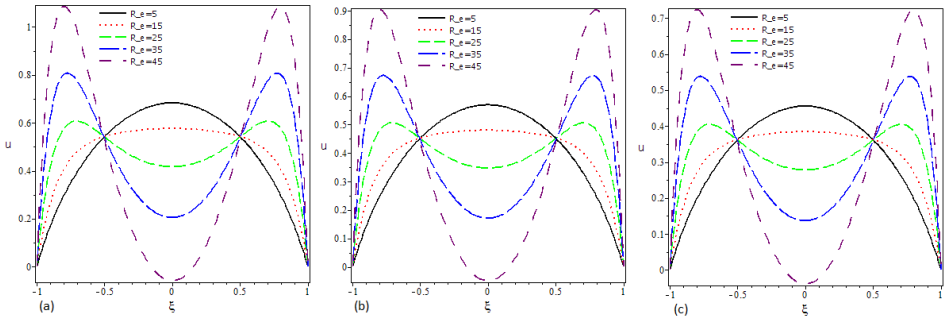

Figure 10. Variation in axial velocity due to R_e when $S = 0.4$, $\delta = 0.2$, at (a) $x = 0.1$, (b) $x = 0.5$, (c) $x = 0.9$

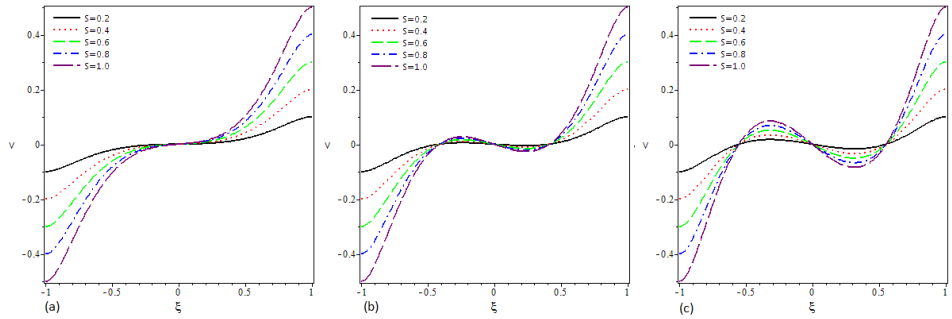

Figure 11. Variation in radial velocity due to absorption for $R_e = 45$, and (a) $\delta = 0.0$ (b) $\delta = 0.4$ (c) $\delta = 0.8$

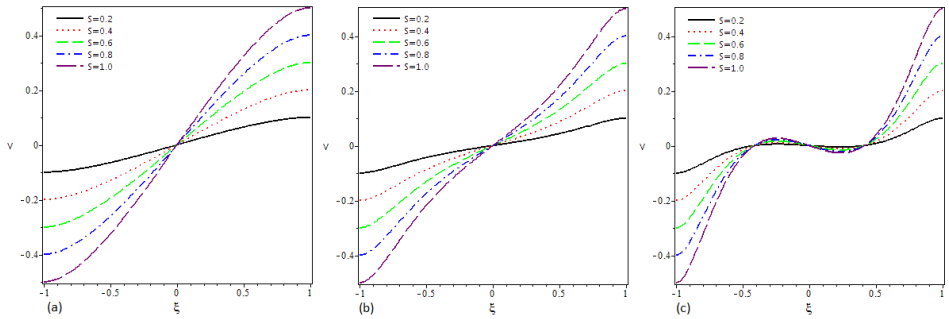

Figure 12. Radial velocity due to variation in S for $\delta = 0.4$ and (a) $R_e = 5$, (b) $R_e = 25$, (c) $R_e = 45$.

In figs. 13(a–c) the streamlines are drawn for Newtonian fluid using different values of S. As we increase absorption, the point where back flow starts, move upstream in the channel.

Figs 14(a–c) are showing the streamlines for Maxwell fluid at different values of δ when $S = 0.4$, $R_e = 45$. As we increase the value of δ, streamlines pattern

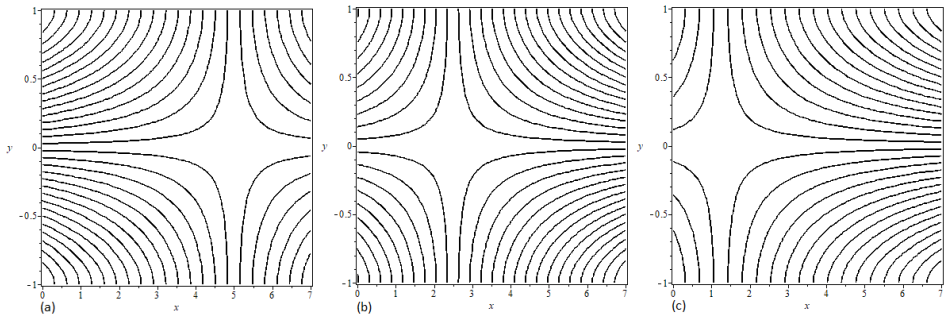

Figure 13. Stream lines for $R_e = 15,\ \delta = 0.0$ (a) $S = 0.2$, (b) $S = 0.4$, (c) $S = 0.8$.

changed due to shear thickening property of the Maxwell fluid. In figs. 15(a–c) variation in streamlines for Maxwell fluid due to R_e is predicted keeping $\delta = 0.4$ and $S = 0.4$.

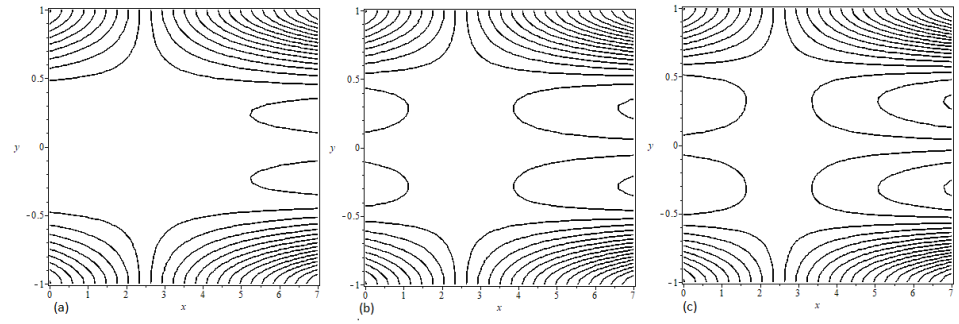

Figure 14. Stream lines for $R_e = 45,\ S = 0.4$ (a) $\delta = 0.4$, (b) $\delta = 0.6$, (c) $\delta = 0.8$.

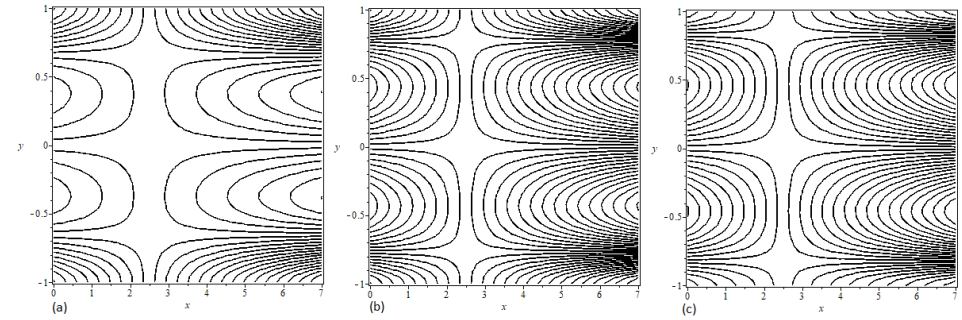

Figure 15. Stream lines for $\delta = 0.4,\ S = 0.4$ (a) $R_e = 60$, (b) $R_e = 80$, (c) $R_e = 100$.

Figs. 16(a–c)–18(a–c) are showing the variations in wall shear stress, τ_w due to different parameters. Fig. 16(a) is showing that when the walls are solid ($S = 0$)

and $R_e = 0$ then τ_w remain constant along the channel. The magnitude of wall shear stress increases with increasing δ. Figs. 16(b–c) are drawn to show the effect in the presence of porosity (i.e., $S = 0.4$) when $R_e = 0$ and $R_e = 15$, respectively. Fig. 16(b) is showing that τ_w is decreasing in x direction with the increase in δ when the walls are porous, even the flow is creeping flow ($R_e = 0$). In the absence of inertial forces (i.e., $R_e = 0$) porosity effects for Newtonian and Maxwell fluids are shown in figs. 17(a,c). From these figs. we can also see that for $R_e = 0, \delta = 0$ results match with the results given in [7]. Figs. 17(a–b) are drawn to analyze the behavior of Newtonian fluid in porous channel with and without inertial forces. It is observed that drop in τ_w can be controlled by decreasing inertial forces. We observe from fig. 18(a) that τ_w for Maxwell fluid decreases along x by increasing S. We have noticed from Fig. 18(b–c) that if δ is increased then τ_w has very high value near the entrance for the same value of R_e but it drop down very fast as compare to its magnitude at low δ.

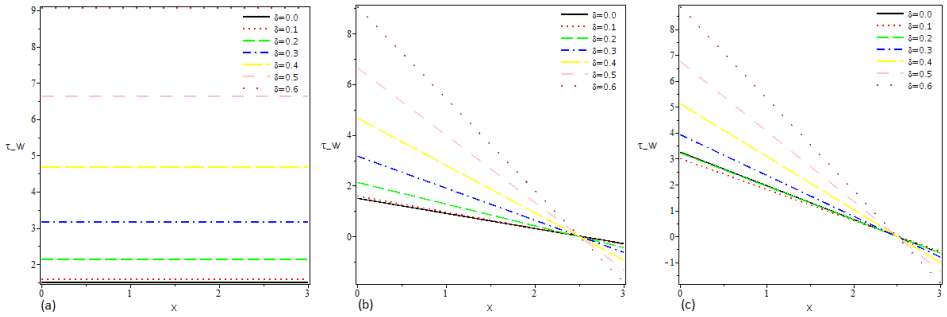

Figure 16. Variation in wall shear stress with δ when (a) $S = 0.0, R_e = 0$, (b) $S = 0.4, R_e = 0$, (c) $S = 0.4, R_e = 15$.

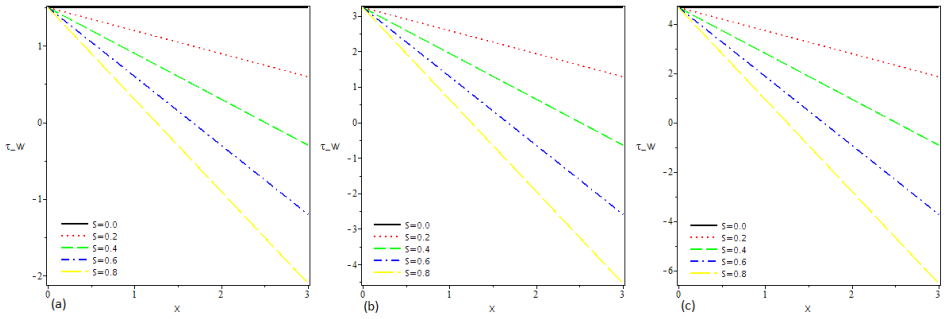

Figure 17. Variation in wall shear stress due to S when (a) $\delta = 0.0, R_e = 0$, (b) $\delta = 0.0, R_e = 15$, (c) $\delta = 0.4, R_e = 0$.

It is noticed from Figs.19(a–c) that porosity has prominent effect on normal stress difference (i.e., τ_n) away from boundaries in Maxwell fluid. τ_n decreases near the boundaries with increasing S. Thickening effect of Maxwell fluid is very obvious in figs. 19(a–b). The effect of S on τ_n is shown in figs. 19(c) and 20(a). The effect of R_e on Maxwell fluid in non-porous channel is depicted in figs. 20(b–c)).

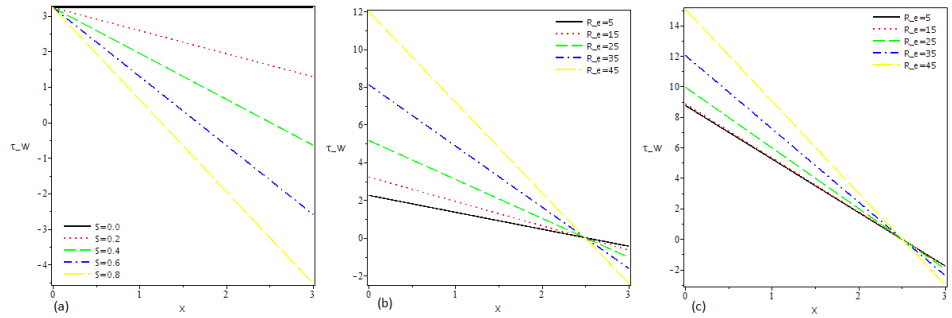

Figure 18. Variation in wall shear stress due to (a) S when $\delta = 0.2, R_e = 15.0$, (b) R_e when $\delta = 0.2, S = 0.4$, (c) R_e when $\delta = 0.6, S = 0.4$,

Pressure difference due to porosity for Newtonian fluid at different R_e are drawn in figs. 21(a–c). As we increase Maxwell material parameter δ in figs. 22(a–c), the pressure drops downstream and have negative value for low Reynolds number (i.e., $R_e = 0.5$) but with increasing R_e, Δp increases down stream and its magnitude becomes positive.

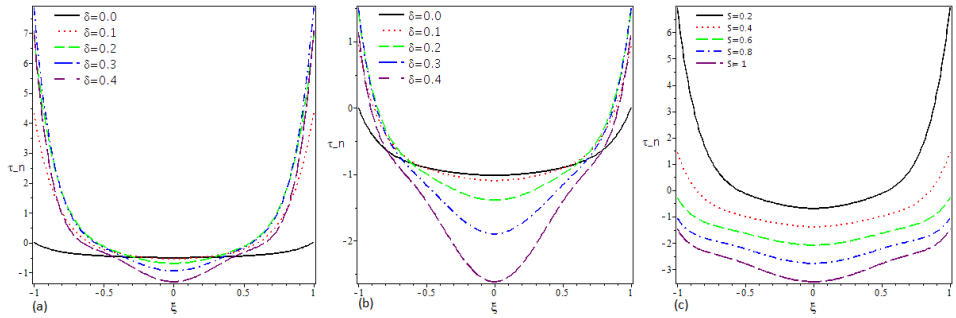

Figure 19. Effect on normal stresses difference of δ when (a) $S = 0.2, R_e = 15$, (b) $S = 0.4, R_e = 15$, and of S when (c) $\delta = 0.2, R_e = 15$,

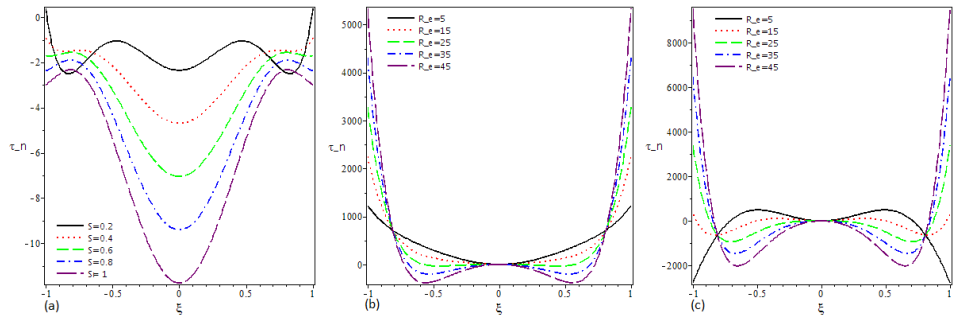

Figure 20. Effect on normal stresses difference of S when (a) $\delta = 0.6, R_e = 15$, and of R_e when (b) $\delta = 0.2, S \to 0$, (c) $\delta = 0.6, S \to 0$.

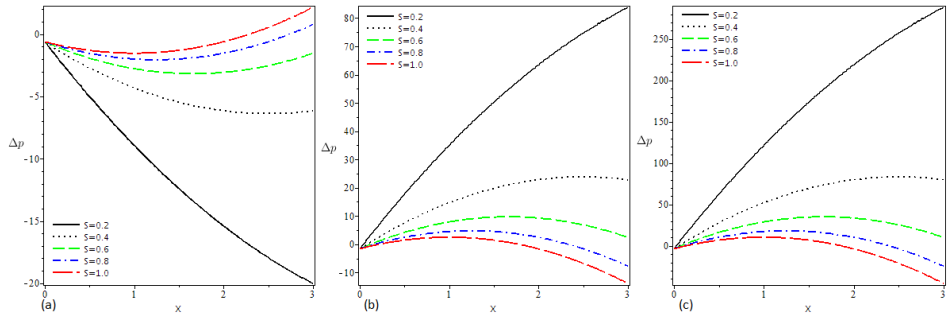

Figure 21. Pressure difference Δp due to S when $\delta = 0$, (a) $R_e = 0.5$, (b) $R_e = 5$, (c) $R_e = 15$.

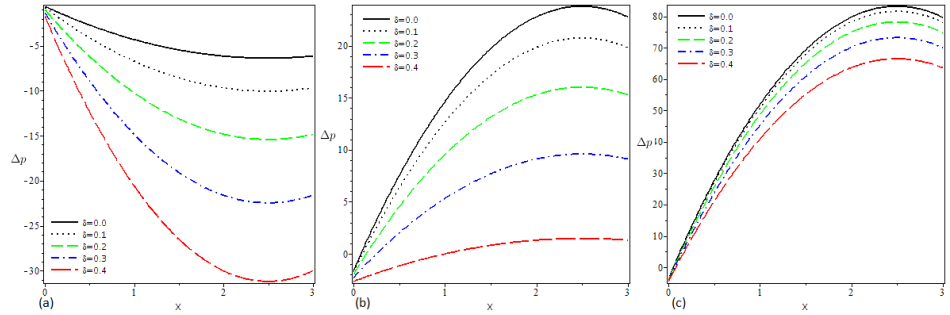

Figure 22. Pressure difference Δp due to δ when $S = 0.4$ (a) $R_e = 0.5$, (b) $R_e = 5$, and (c) $R_e = 15$.

References

[1] Z. Abbas, S. Rafiq and M. Sheikh, *Oscillatory darcy flow of Non-Newtonian Casson fluid with temperature dependent viscosity in a porous channel*, Arab. J. Sci. Eng., 2020, 45, 7247–7255.

[2] S. Ahmad, M. Ashraf and K. Ali, *Simulation of thermal radiation in a micropolar fluid flow through a porous medium between channel walls*, J. Therm. Anal. Calorim., 2020, 1–13.

[3] A. S. Berman, *Laminar flow in channels with porous walls*, J. Appl. Phys., 1953, 24, 1232–1235.

[4] S. M. Cox, *Two-dimensional flow of a viscous fluid in a channel with porous walls*, J. Fluid Mech., 1991, 227, 1–33.

[5] J. J. Choi, Z. Rusak and J. A. Tichy, *Maxwell fluid suction flow in a channel*, J. non-Newtonian Fluid Mech., 1999, 85, 165–187.

[6] D. D. Ganji and A. Sadighi, *Application of He's homotopy perturbation method to nonlinear coupled systems of reaction-diffusion equations.*, Int. J. Nonlin. Sci., 2006, 7, 411–418.

[7] T. Haroon, A. M. Siddiqui and A. Shahzad, *Creeping Flow of Viscous Fluid through a Proximal Tubule with Uniform Reabsorption: A Mathematical Study*, Appl. Math. Sci., 2016, 10(16), 79–807.

[8] Q. Huang, L. Li and Z. Ouyang, *Asymptotic solutions on multiple solutions arising from laminar flow in a uniformly porous channel with expanding or contracting walls*, Bound. Value Prob., 2019, 39, 1–15.

[9] F. Irgens, *Rheology and Non-Newtonian Fluids*, Springer International Publishing Switzerland, 2014, 162.

[10] M. Kahshan, D. Lu and A. M. Siddiqui, *A Jeffrey fluid model for a porous walled channel: application to flat plate dialyzer*, Sci. Rep., 2019, 9, 15879.

[11] D. Lu, M. Kahshan and A. M. Siddiqui, *Hydrodynamical study of Micropolar fluid in a porous walled channel, Application to flat plate dialyzer*, Symmetry, 2019, 11, 541.

[12] W. E. Langlois, *Steady flow of slightly visco-elastic fluids*, PhD Thesis, Brown University, 1957.

[13] W. E. Langlois, *The recursive theory of slow viscoelastic flow applied to three basic problems of hydrodynamics*, Trans. Soc. Rheol., 1964, 8, 33–60.

[14] R. Larson, *Constitutive equations for polymer melts and solutions*, Boston, Butterworths, 1988.

[15] J. C. Maxwell, *On the dynamical theory of gases*, Philosophical Transactions of the Royal Society London, 1866, A157, 26–78.

[16] M. Rashevski and S. Slavtchev, *Heat transfer in laminar viscous flow in a channel with one porous wall*, Eur. J. Mech., 2020, 82, 11v20.

[17] K. R. Rajagopal and A. R. Srinivasa, *A thermodynamic frame work for rate type fluid models*, J. Non-Newtonian Fluid Mech., 2000, 88, 207–227.

[18] A. Rajabi, D. D. Ganji and H. Taherian, *Application of homotopy perturbation method in nonlinear heat conduction and convection equations*, Phys. Lett. A., 2007, 360, 570v573.

[19] A. M. Siddiqui, T. Haroon and M. Kahshan, *MHD flow of Newtonian fluid in a permeable tubule*, Magnetohydrodynamics, 2015, 51(4), 655–672.

[20] A. M. Siddiqui, T. Haroon and A. Shahzad, *Hydrodynamics of viscous fluid through porous slit with linear absorption*, Appl. Math. Mech. Engl. Ed., 2016, 37(3), 361v378.

[21] K. Sadeghy, A. H. Najafi and M. Saffaripour, *Sakiadis flow of an upper convected Maxwell fluid*, Int. J. non-Linear Mech., 2005, 40, 1220–1228.

[22] M. G. Sobamowo, *Singular perturbation and differential transform methods to two-dimensional flow of nanofluid in a porous channel with expanding/contracting walls subjected to a uniform transverse magnetic field*, Therm. Sci. Eng. Prog., 2017, 4, 71–84.

[23] R. M. Terrill, *Laminar flow in a uniformly porous channel*, Aeronaut. Quart., 1964, 15, 299–310.

[24] R. M. Terrill, *Laminar flow in a uniformly porous channel with large injection*, Aeronaut. Quart., 1965, 16, 323–332.

[25] W. Tan and M. Xu, *Plane surface suddenly set in a motion in viscoelastic fluid with fractional Maxwell model*, Acta Mech. Sinica, 2002, 18, 343–348.

[26] H. Ullah, D. Lu, A. M. Siddiqui, T. Haroon and K. Maqbool, *Hydrodynamical study of creeping Maxwell Fluid flow through a porous slit with uniform reabsorption and wall slip*, Mathematics, 2020, 8, 1852.

[27] H. Ullah, H. Sun, A. M. Siddiqui and T. Haroon, *Creeping flow analysis of slightly non-Newtonian fluid in a uniformly porous slit*, J. Appl. Anal. Comput., 2019, 9(1), 140v158.

[28] H. Ullah, A. M. Siddiqui, H. Sun and T. Haroon, *Slip effects on creeping flow of slightly non-Newtonian fluid in a uniformly porous slit*, J. Braz. Soc. Mech. Sci., 2019, 41, 412.

[29] S. Yuan, *Further investigation of laminar flow in channels with porous walls*, J. Appl. Phys., 1956 27, 267–269.